

SUPPLEMENTARY INFORMATION

Tumor-intrinsic PIK3CA Represses Tumor Immunogenicity in a Model of Pancreatic Cancer

Running title: Pik3ca and pancreatic cancer immune evasion

Nithya Sivaram^{1,2}, Patrick A. McLaughlin³, Han V. Han^{1,4}, Oleksi Petrenko³, Ya-Ping Jiang¹, Lisa M. Ballou¹, Kien Pham⁵, Chen Liu⁵, Adrianus W.M. van der Velden³, and Richard Z. Lin^{1,6}

¹Department of Physiology and Biophysics, Stony Brook University, Stony Brook, N.Y.

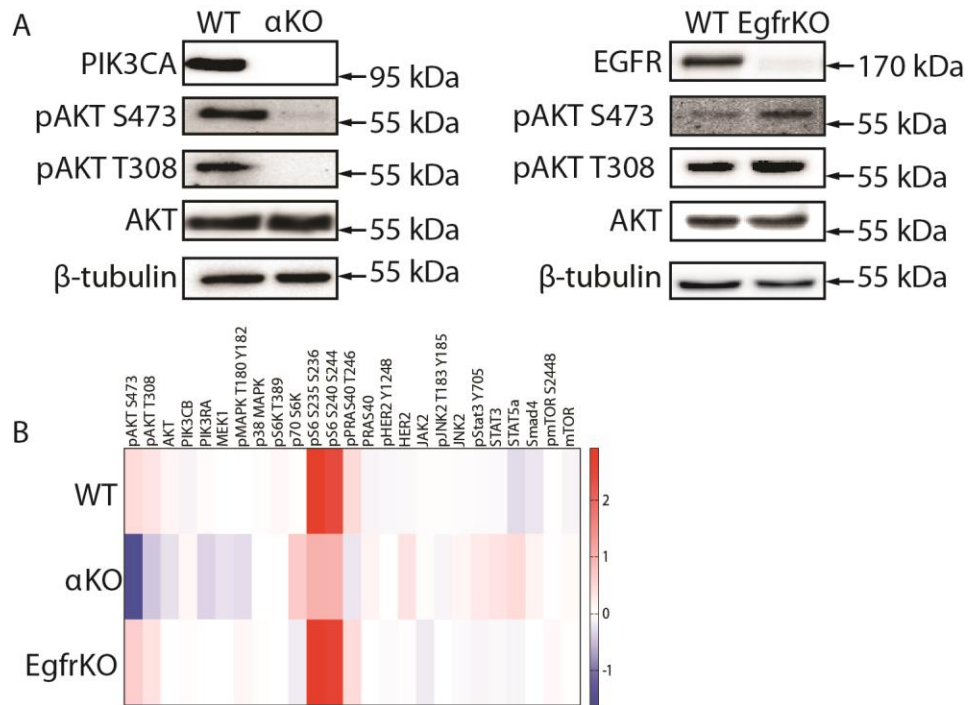
²Molecular and Cellular Biology Graduate Program, Stony Brook University, Stony Brook, N.Y.

³Department of Molecular Genetics and Microbiology and Center for Infectious Diseases, Stony Brook University, Stony Brook, N.Y.

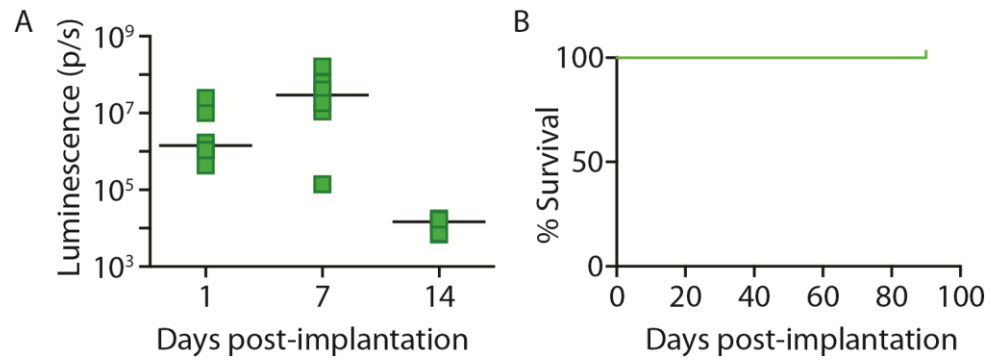
⁴Biomedical Engineering Graduate Program, Stony Brook University, Stony Brook, N.Y.

⁵Department of Pathology and Laboratory Medicine, New Jersey Medical School and Robert Wood Johnson Medical School, Rutgers University School of Medicine, Newark, N.J.

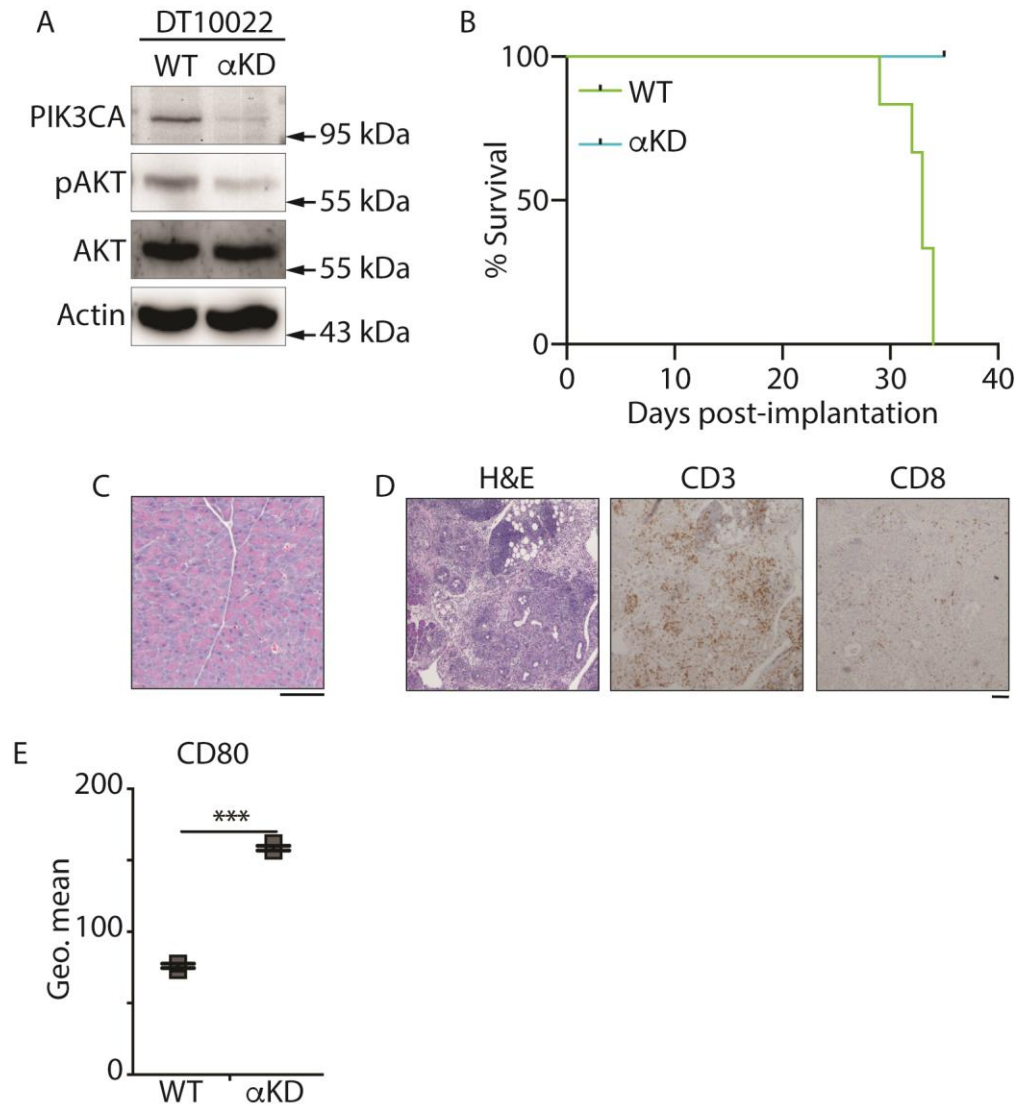
⁶Medical Service, Northport VA Medical Center, Northport, N.Y.



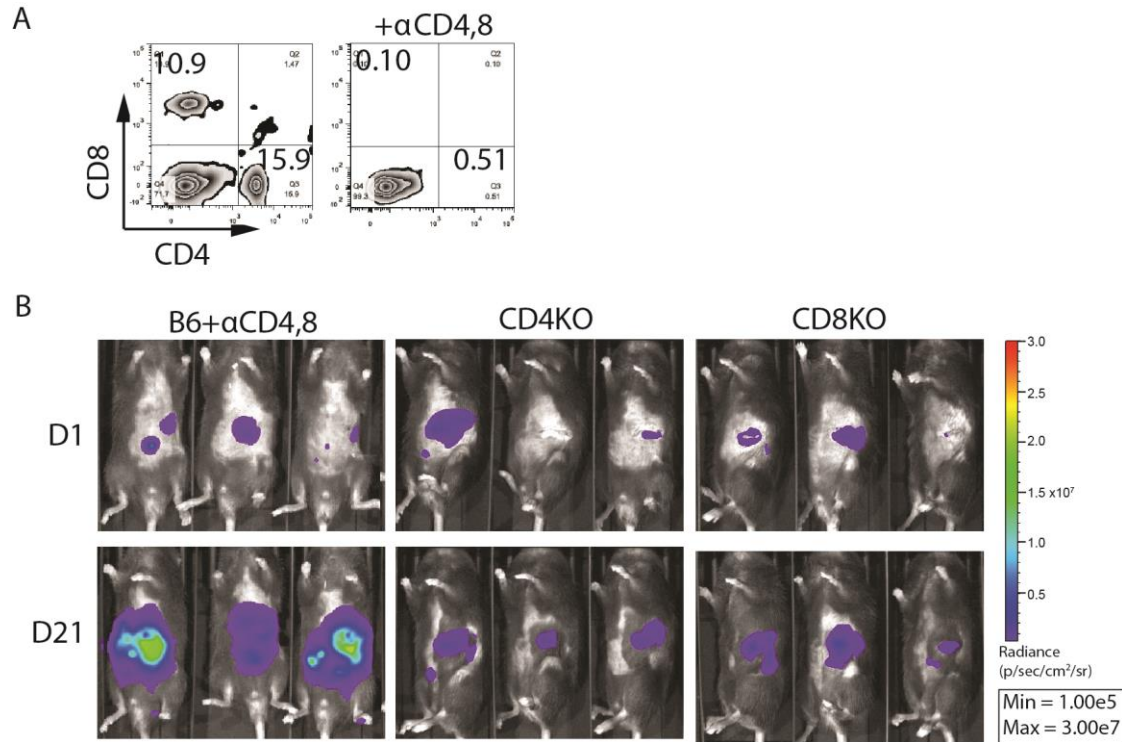
Supplementary Fig. S1. Western blotting and RPPA analysis of KPC cell lines. *Pik3ca* or *Egfr* were targeted in wildtype (WT) KPC cells using CRISPR/Cas9 and clonal cell lines were established. **(A)** Representative western blots to confirm gene ablation and to assess AKT activation. β tubulin is a loading control. Experiments were repeated 3 times. **(B)** Heatmap for RPPA analysis of the three cell lines.



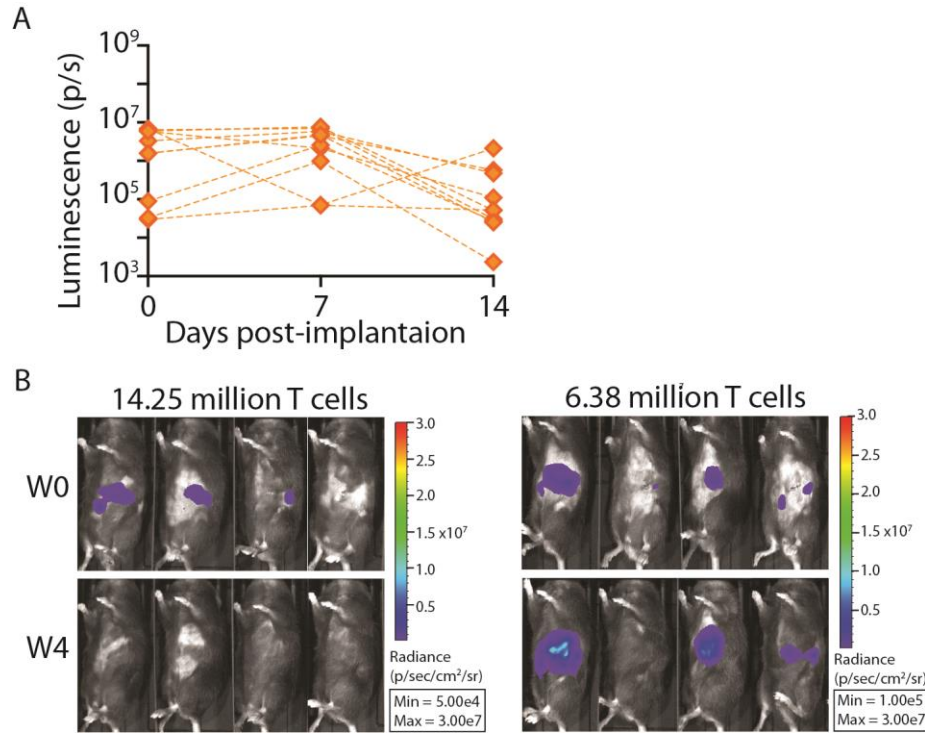
Supplementary Fig. S2. Regression of α KO clone2 tumors *in vivo*. α KO clone2 cells (0.5 million) were implanted in the head of the pancreas of B6 mice ($n = 6$) and tumor growth was monitored by IVIS imaging of the luciferase signal. **(A)** Graph shows quantification of luciferase signals. **(B)** Kaplan-Meier survival curve.



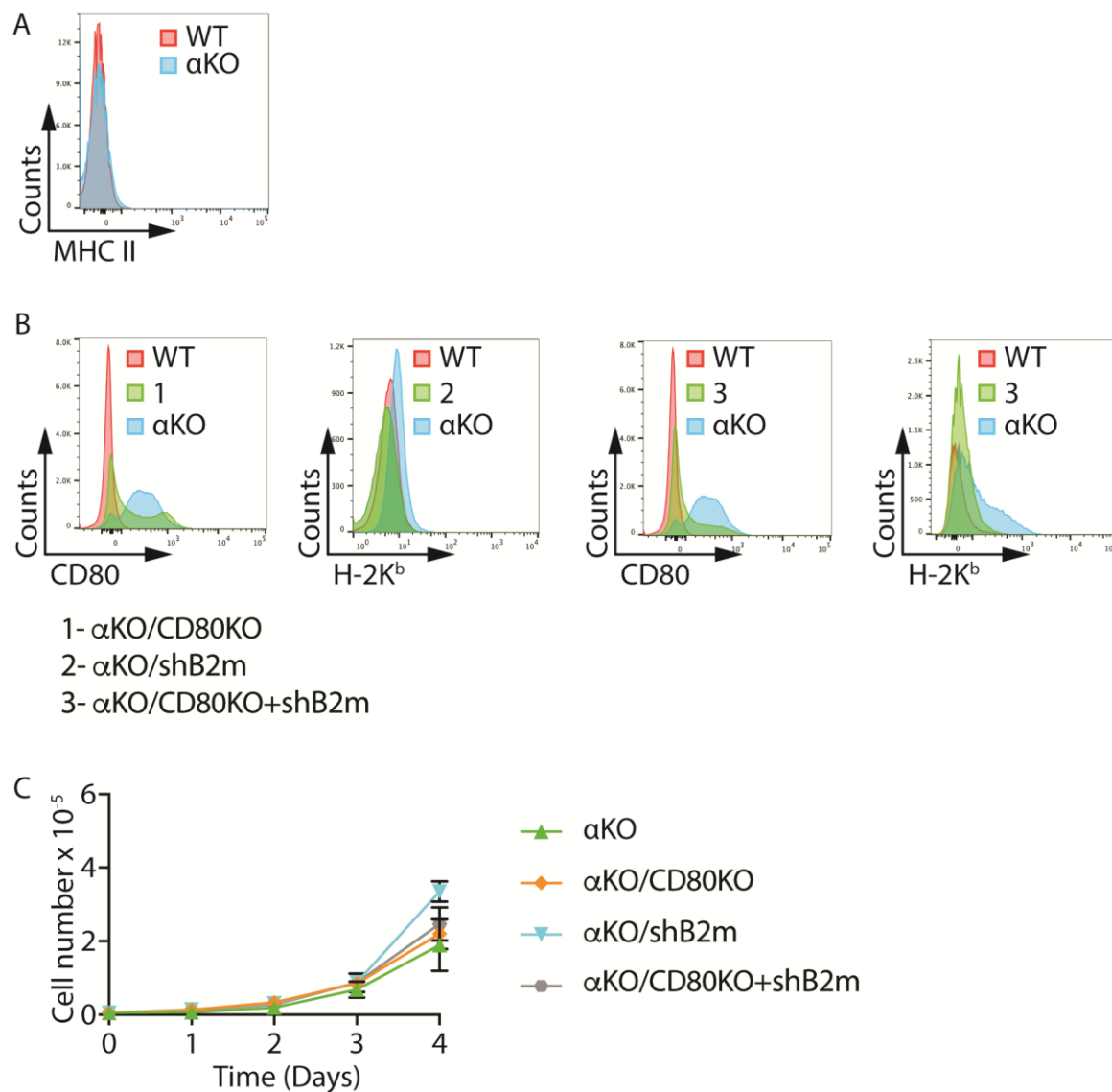
Supplementary Fig. S3. *In vitro* and *in vivo* characterization of α KD cells. *Pik3ca* was targeted in DT10022 cells using CRISPR/Cas9, and clonal cell line α KD was established. **(A)** Western blotting analysis shows a reduction in PIK3CA and pAKT levels in α KD cells as compared to WT DT10022 cells. Actin is a loading control. **(B)** Kaplan-Meier survival curves for B6 mice implanted with WT or α KD cells (0.5 million) in the head of the pancreas ($n = 6$). $P = 0.0008$ (log-rank test). **(C)** Mice implanted with α KD cells in **B** were euthanized 35 days after implantation. H&E-stained pancreatic section from a mouse with no tumor. Scale bar, 100 μ m. **(D)** 0.5 million α KD cells were implanted in the head of the pancreas of B6 mice and pancreata were harvested 10 days later. Sections were stained with H&E, or IHC was performed with the indicated antibodies. Representative sections are shown. $n = 3$. Scale bar, 100 μ m. **(E)** Cell surface CD80 levels in WT and α KD cells as determined by flow cytometry. The mean \pm SEM of the geometric means (Geo. Mean) of each flow cytometry distribution is shown ($n = 3$). *** $P = 0.0004$ (paired t -test).



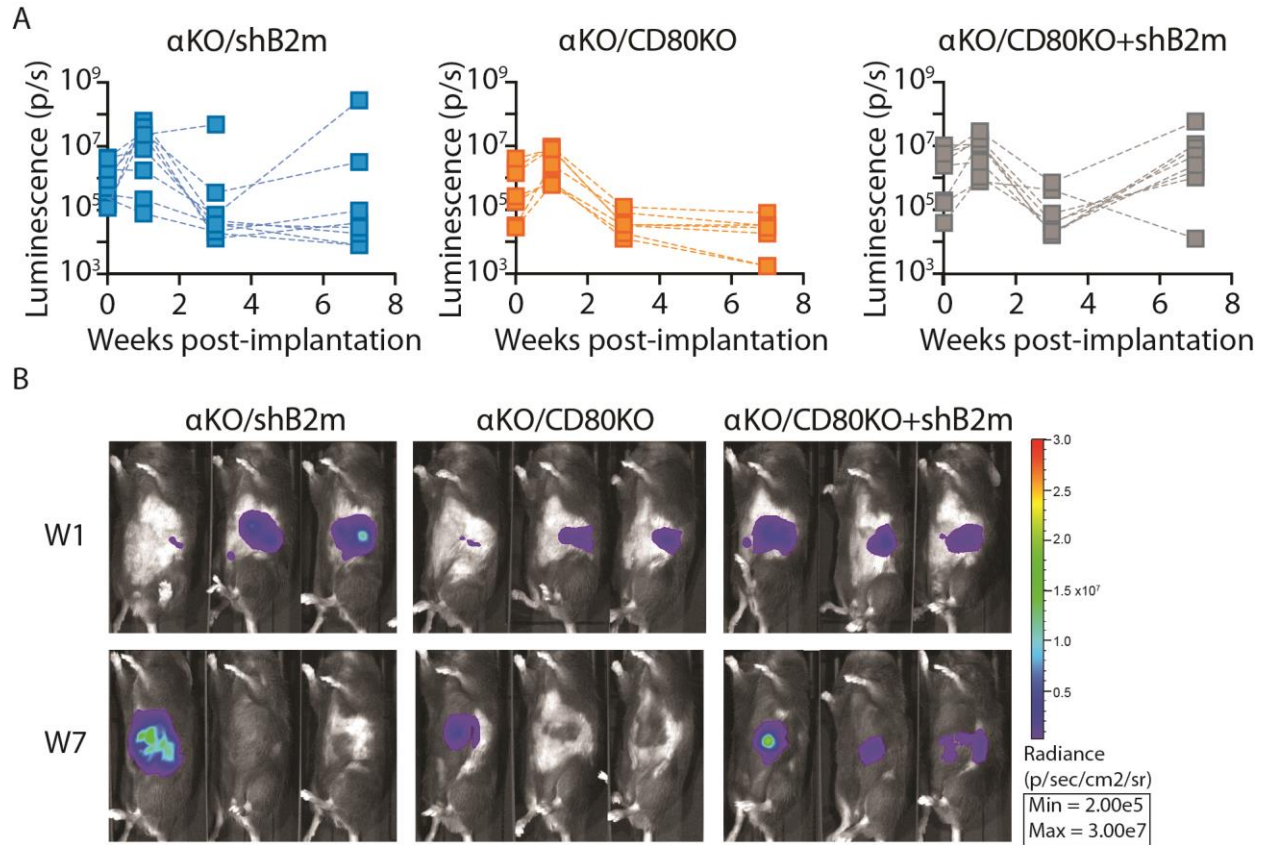
Supplementary Fig. S4. Tumor growth in mice lacking CD4 and/or CD8 T cells. (A) B6 mice were injected with neutralizing CD4 and CD8 antibodies. Peripheral blood was analyzed by flow cytometry to detect depletion of CD4⁺ and CD8⁺ T cells. Dot plots show CD4⁺ and CD8⁺ T cells in mice injected with saline (*left*) or CD4/8 antibodies (*right*). **(B)** IVIS images of B6 mice injected with CD4/8 antibodies, CD4KO mice, and CD8KO mice implanted with 0.5 million α KO cells in the head of the pancreas.



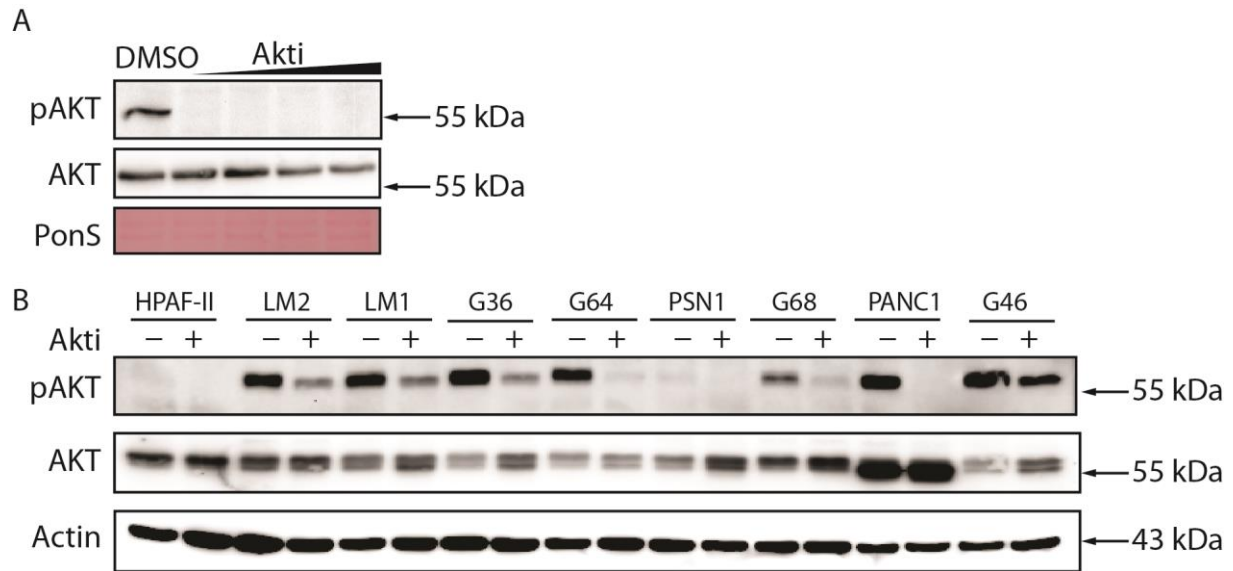
Supplementary Fig. S5. α KO tumor regression in SCID mice treated with T cells. **(A)** Mice were implanted with 0.5 million α KO KPC cells 24 hours after adoptive transfer of T cells from a convalescent B6 mouse previously implanted with α KO cells. Quantification of luciferase signals from each mouse. $n = 8$. **(B)** 0.5 million α KO KPC cells were implanted in the head of the pancreas of SCID mice ($n = 8$). Four days later, the mice were imaged ($t = W0$) and then treated with 14.25 million or 6.38 million T cells ($n = 4$ per group) from a convalescent B6 mouse previously implanted with α KO cells. IVIS images show luciferase signals as a measure of tumor volume before and 4 weeks after treatment.



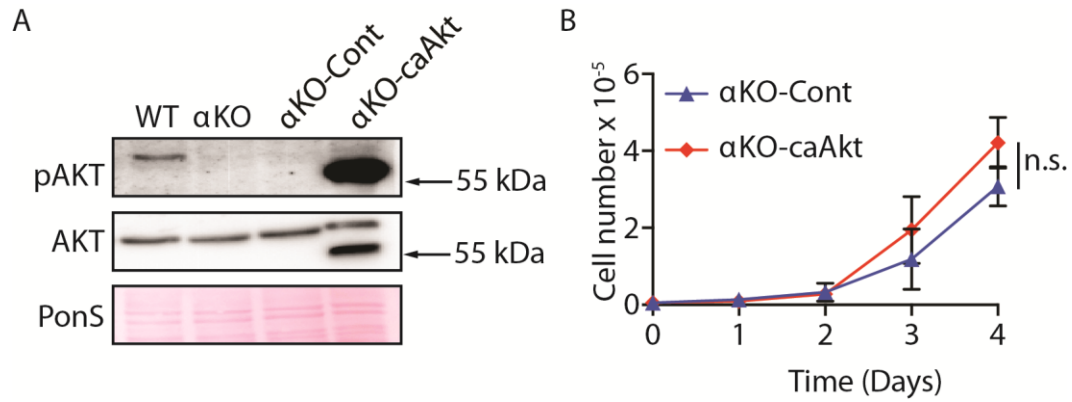
Supplementary Fig. S6. Cell surface levels of MHC II, H-2K^b, and CD80 in KPC cell lines. Flow cytometric analysis to determine levels of **(A)** MHC II (I-A^b) and **(B)** H-2K^b and CD80. **(C)** Proliferation rates of α KO KPC cell lines in standard 2D culture. Cells plated in triplicate were counted at the times indicated (mean \pm SEM; $n = 3$). The three cell lines grew at rates similar to α KO cells (One-way ANOVA with Bonferroni's multiple comparison's test).



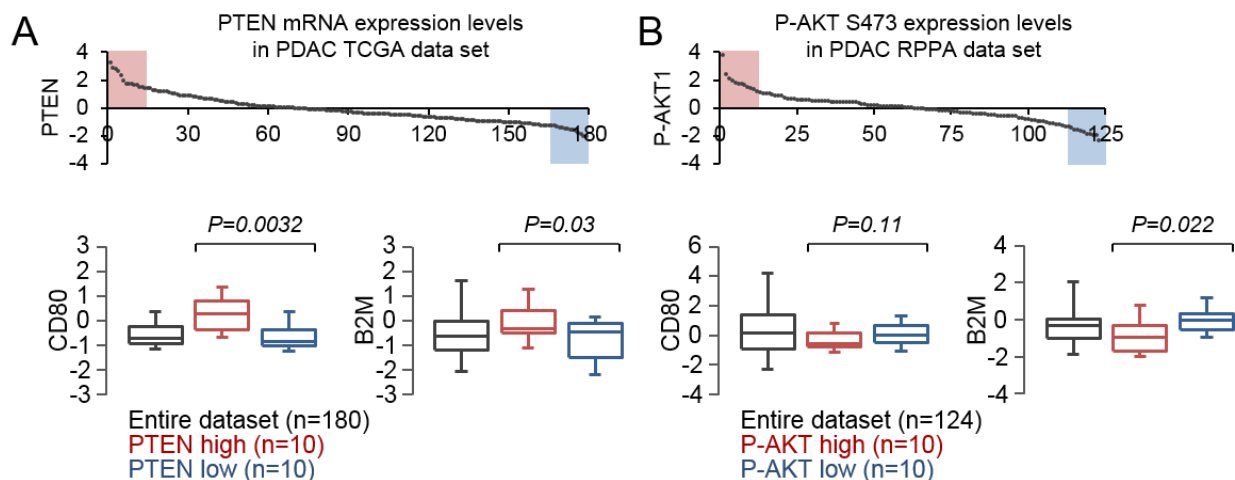
Supplementary Fig. S7. *In vivo* tumor growth. B6 mice were implanted with 0.5 million αKO/shB2m, αKO/CD80KO, or αKO/CD80KO+shB2m cells in the head of the pancreas, and tumor growth was monitored by IVIS imaging. **(A)** Quantification of the luciferase signals in each mouse. αKO/shB2m, $n = 8$; αKO/CD80KO, $n = 7$; αKO/CD80KO+shB2m, $n = 8$. **(B)** Representative images of 3 mice in each group are shown.



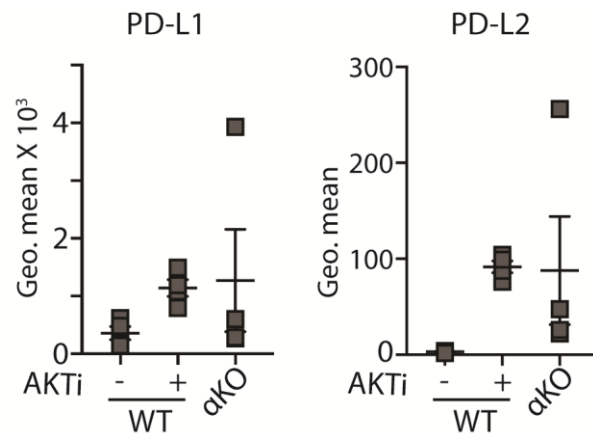
Supplementary Fig. S8. Effect of Akti treatment on phospho-AKT. (A) WT KPC cells were treated with increasing concentrations of Akti or (B) human PDAC cell lines were treated with 10 μ M Akti for 48 hours. Cells were lysed in RIPA buffer and total protein was run on a denaturing gel. Western blots show levels of phospho- and total AKT. Actin in a loading control. PonS, Ponceau S-stained blot.



Supplementary Fig. S9. AKT phosphorylation and *in vitro* growth of α KO-caAkt cells. (A) α KO cells were infected with lentivirus expressing control vector (Cont) or caAkt. Western blots confirm the expression of caAkt. PonS, Ponceau S-stained blot. **(B)** Proliferation rates in standard 2D culture. Cells plated in triplicate were counted at the times indicated (mean \pm SEM; $n = 3$). n.s., not significant.



Supplementary Fig. S10. Correlation between PIK3CA/AKT signaling and expression of CD80 and B2M in PDAC patients. The Cancer Genome Atlas (TCGA) data were downloaded as z-scores from the cBioPortal (<http://www.cbioportal.org>). RNAseqV2 data were available for PTEN, CD80 and B2M. The RPPA data contain phospho-AKT1 levels. **(A)** *Top*, range of PTEN mRNA expression levels in the PDAC data set. Shading shows 10 samples with high (pink) or low (blue) PTEN expression. *Bottom*, box plots comparing CD80 and B2M mRNA levels in patients with high or low PTEN expression (Student's *t*-test). **(B)** *Top*, range of phospho-AKT1 S473 expression levels in the PDAC data set. Shading shows 10 samples with high (pink) or low (blue) phospho-AKT expression. *Bottom*, box plots comparing CD80 and B2M mRNA levels in patients with high or low phospho-AKT levels (Student's *t*-test).



Supplementary Fig. S11. Cell surface levels of PD-L1 and PD-L2 in WT and α KO cells.

WT KPC cells were treated with 10 μ M Akti for 48 hours. Cell surface levels of PD-L1 and PD-L2 were quantified by flow cytometry. WT cells treated with DMSO and α KO cells were used for comparison. The graph shows the mean \pm SEM of the geometric means (Geo. Mean) of each flow cytometry distribution. $n = 4$. The data did not reach statistical significance (One-way ANOVA with Bonferroni's post hoc test).

A

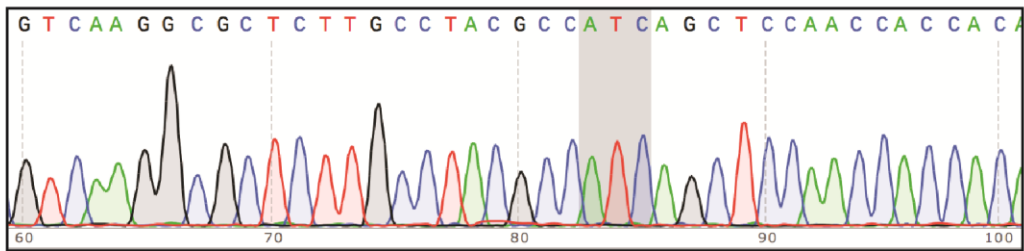
```

mKras -----aggcctgctgaaaatgactgag
KPC  ATGTTCTAATTTAGTTGTATTTTATTATTTTATTGTAAGGCCTGCTGAAAATGACTGAG

mKras  tataaacttggtggtggttgagctggcgtaggcaagagcgccttgacgatacagcta
KPC  TATAAGCTTGTGGTGGTGGAGCTGATGGCGTAGGCAAGAGCGCCTTGACGATACAGCTA

mKras  attcagaatcactttgtggatgagtatgaccctacgatagaggactcctacaggaaacaa
KPC  ATTCAGAATCACTTTGTGGATGAGTA-----
  
```

B



Supplementary Fig. S12. Sequence of *Kras* exon 1. Genomic DNA from WT KPC cells was used for sequencing exon 1 of the *Kras* gene. **(A)** Sequence alignment of DNA from KPC cells (KPC) against the murine *Kras* gene (NCBI Gene ID 16653) (*mKras*). **(B)** Chromatogram showing G12D mutation (grey highlight) in WT KPC cells.